Light-scattering properties beyond weak-field excitation in atomic ensembles

Chung-Hsien Wang,[1,2,*] Nai-Yu Tsai,[3] Yi-Cheng Wang,[4] and H. H. Jen[1,5,†]
[1]*Institute of Atomic and Molecular Sciences, Academia Sinica, Taipei 10617, Taiwan*
[2]*Department of Physics, National Taiwan University, Taipei 10617, Taiwan*
[3]*Department of Physics and Astronomy, Stony Brook University, Stony Brook, New York 11794, USA*
[4]*Department of Physics, University of California, Berkeley, Berkeley, California 94720, USA*
[5]*Physics Division, National Center for Theoretical Sciences, Taipei 10617, Taiwan*

(Received 25 October 2023; revised 29 May 2024; accepted 1 July 2024; published 22 July 2024)

In the study of optical properties of large atomic systems, a weak laser driving is often assumed to simplify the system dynamics by linearly coupled equations. Here we investigate the light-scattering properties of atomic ensembles beyond weak-field excitation through the cumulant expansion method. By progressively incorporating higher-order correlations into the steady-state equations, an enhanced accuracy can be achieved in comparison to the exact solutions obtained by solving a full density matrix. Our analysis reveals that, in the regime of weak dipole-dipole interaction, the first-order expansion yields satisfactory predictions for optical depth, while denser atomic configurations necessitate consideration of higher-order correlations. As the intensity of incident light increases, atom saturation effects become noticeable, giving rise to significant changes in light transparency, energy shift, and decay rate. This saturation phenomenon extends to subradiant atom arrays even under weak driving conditions, leading to substantial deviations from the linear model. Our findings demonstrate that the mean-field model is a good extension to linear models as it balances both accuracy and computational complexity. However, the crucial role of higher-order cumulants in large and dense atom systems remains unclear, since it is challenging theoretically owing to the exponentially increasing Hilbert space in such light-matter interacting systems.

DOI: 10.1103/PhysRevA.110.013708

I. INTRODUCTION

The interaction between light and atoms stands as one of the most fundamental phenomena in physics. Its existence extends to atoms, molecules, and solids [1–3], playing a crucial role in modern physics. Such an interaction has many interesting effects. When light interacts with atoms, a pairwise and resonant dipole-dipole interaction (RDDI) emerges through multiple light scatterings among the atoms [4]. This pairwise interaction between atoms can result in intriguing properties as the number of atoms increases or under some specific spatial structure [5]. The complexities from the number of atoms, ensemble geometry, and interaction forms significantly influence the optical properties of atom ensembles, giving rise to phenomena like superradiance [6–9], subradiance [10–23], and even resonant frequency shifts [24–27]. All of these collective radiation properties signify a difference from the behavior of individual atoms and result in pronounced deviations from the classical Beer-Lambert law [28]. The precise manipulation of this interaction bears the potential for numerous applications across various domains, including nanophotonics [29], quantum technology [30,31], and materials science [32,33].

Utilizing a group of atoms to interact with light presents one of the ways to probe the RDDI and investigate the validity of theories in quantum optics. Through the well-developed laser control and atom trapping technique [34,35], a variety of systems can be effectively explored by measuring distinct system dynamics of various platforms, for example, the analysis of scattering spectra [36,37] and optical depth [38]. This further facilitates the examination of atomic optical properties in various geometries, such as randomly distributed samples [39], quasi-two-dimensional slabs [40], and ordered arrays [22,41]. In the pursuit of the strong-coupling regime of light-matter interactions, the atoms can be put inside a cavity [42] or close to the waveguide [43].

While the theoretical analysis of atomic dynamics under RDDI is well established in few-atom cases, the exact dynamics of a large atomic system remains, however, a challenge to computations due to an exponential growth of accessible Hilbert space. To deal with this difficulty, a regime of weak driving strength is often employed. Under such conditions, atoms experience only a modest level of excitation and thus populate mostly in the ground states. In this way the system dynamics can be simplified and reduced to coupled linear equations allowing efficient computation. This linear model has been studied theoretically [44–46] and examined in many experiments [9,47,48]. However, this assumption could be too idealized, although theoretically correct under the weak-excitation regime, and might fall short in practice due to finite driving strength [49]. This issue arises due to the

*Contact author: b07202032@ntu.edu.tw
†Contact author: sappyjen@gmail.com

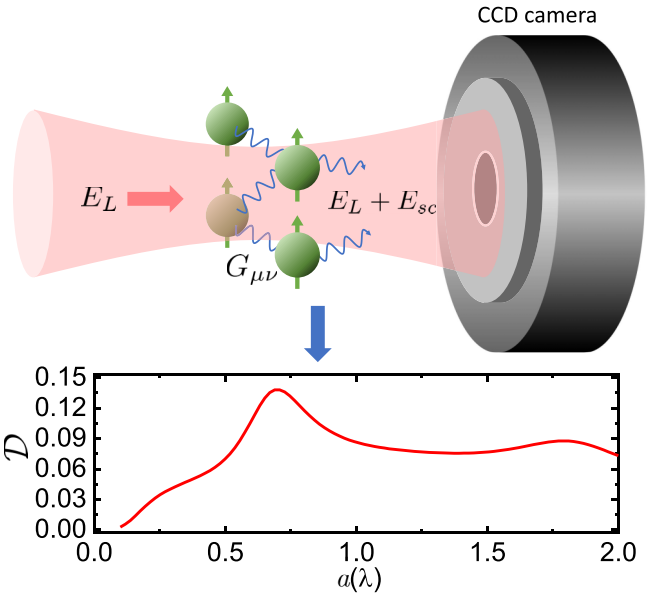

FIG. 1. Schematic diagram of the experimental device measuring an atomic ensemble's optical depth. The input laser field E_L drives atoms and induces RDDI among them with strength $G_{\mu\nu}$. The output field $E_L + E_{sc}$ containing the input laser field plus the atoms' dipole radiation E_{sc} is collected by the CCD camera on the right-hand side. By comparing the field input-output ratio, we can calculate the transmission coefficient $\mathcal{T}$ as well as optical depth $\mathcal{D} = -\ln|\mathcal{T}|^2$ of a given ensemble. For example, the plot below shows the optical depth of the 2×2 array for different lattice spacings a, the laser is chosen to be resonant, and $\Omega_0 = 0.1\Gamma$, with an injection direction perpendicular to the plane of the array.

non-negligible effects of finite atomic excitation and quantum correlations between atoms via RDDI [50]. To go beyond weak-field approximation and include the effect of quantum correlations among the atoms, a cumulant expansion method [51] can be adopted. By truncating many-body correlations by finite orders, a more controllable and precise calculation can be performed, depending on the selected truncation order [52]. This method has demonstrated its utility in investigating the dynamics of superradiance from totally inverted systems [53] and chiral waveguides [54].

In this work we study the optical properties of atoms distributed in free space. As shown in Fig. 1, atoms are driven by a laser and interact through RDDI until they reach steady states. We note that we are considering a free-space RDDI, which differs from the setup described in [54], where a one-dimensional chiral atom-waveguide interface was considered. Additionally, our study focuses on a driven atomic system, as opposed to the decaying inverted system in [53]. Scattered fields together with coherent drive are collected by a camera in the far field. By comparing the ratio of these fields in the presence and absence of atoms, the optical depths are obtained. In experimental realizations, the ^{87}Rb atoms' hyperfine states with D_1 or D_2 transitions can serve as two-level systems. The atomic density and the laser focused waist are capable of reaching subwavelength scales [40,41,47]. The atomic configurations can be either high density clouds [24] or subwavelength ordered arrays [41]. These provide us with a benchmark for studying the system with feasible physical parameters. We calculate the atomic steady state through the cumulant expansion method and find that the presence of excited-state populations and the influence of many-body correlations induce substantial deviations from the linear model, particularly in subradiant atomic configurations. This departure from linearity arises from atom saturation effects which limit the atoms' capacity to absorb additional photons and thus results in the emergence of light transparency. Our results provide insight for studying various system parameter regimes, where higher-order cumulants are useful for more-precise light-scattering properties.

The remainder of the paper is organized as follows. In Sec. II we introduce the system's master equation with photon-mediated dipole-dipole interactions and explain the cumulant expansion method. We compare the results by the cumulant expansion method with the exact ones and calculate the relative errors to identify the importance of the order of quantum correlations in the system. In Sec. III we further explore the effect of multiexcitation, which becomes significant when the driving field or the atomic density increases. We then extend our analysis to large atomic arrays, where we find that the cumulant expansion method presents a significant deviation from the linear model even in the weak driving region. We summarize and discuss our conclusions in Sec. IV.

II. CUMULANT EXPANSION METHOD

We start with a system of N identical two-level atoms whose ground and excited states are denoted by $|g\rangle$ and $|e\rangle$, respectively. Here the atoms' dipole polarization is set in the x direction. Atoms are driven by a coherent drive $\mathbf{E}_L(\vec{r}) = E_L e^{-ikz} f(\vec{r})\hat{\mathbf{x}}$ propagating in the z direction and polarized in the x direction. Here $k \equiv 2\pi/\lambda$, with λ the atomic wave vector and the transition wavelength, respectively. In this work we consider a Gaussian beam profile $f(\vec{r}) \sim e^{-(x^2+y^2)/w_0^2}$, with w_0 the focus of the width on the atom sample. We choose the width to be $w_0 = 2.5\lambda$. The transmission coefficient $\mathcal{T}$ of an atomic array is connected to the expectation value of the steady-state transition rate of the μth atom $\langle\sigma_\mu\rangle$ by [28,46]

$$\mathcal{T} = 1 + i\frac{3\Gamma}{\Omega_0 w_0^2 k^2}\sum_{\mu=1}^{N}\langle\sigma_\mu\rangle e^{-ikz_\mu}, \tag{1}$$

where Γ quantifies the atomic spontaneous decay rate and $\sigma_\mu \equiv |g\rangle_\mu\langle e|$ is the lowering operator. This expression indicates the ratio of the sum of all dipole radiations E_{sc} collected by the camera located far away to the driving field E_L. Here $\Omega_0 = 2dE_L$ is the central Rabi frequency, with d the transition dipole moment. We require the camera to be located far enough to ensure that the dipole radiations are in the far-field regime. Within this regime, the strength of dipole radiations decays as fast as the Gaussian beam and can be approximated as if it radiates predominantly parallel to the $\hat{z}$ axis. This approximation results in a distance-independent transmission coefficient that emerges as the second term in Eq. (1). Once $\mathcal{T}$ is obtained, the optical depth can also be calculated by

$\mathcal{D} = -\ln|\mathcal{T}|^2$, which we obtain throughout the paper as the measurable light-scattering property.

Equation (1) establishes a connection between only the atomic dipole moment and the optical depth. The distribution of the dipole moments, however, needs to be solved separately, depending on the effective model. To calculate the atomic dipole and thereby obtain the light response from the light scattering within the atomic system, the master equation for the atoms involves the coherent driving field and the resonant dipole-dipole interactions being considered [4], which reads

$$\frac{d}{dt}\rho = -\frac{i}{\hbar}[H_L, \rho] + \sum_{\mu,\nu=1}^{N} G_{\mu\nu}[\sigma_\mu^\dagger, \sigma_\nu \rho] + G_{\nu\mu}^*[\rho\sigma_\mu^\dagger, \sigma_\nu]. \tag{2}$$

Here ρ denotes the density matrix of N identical two-level atomic systems and H_L is the laser driving Hamiltonian

$$H_L = -\frac{\hbar}{2}\sum_{\mu=1}^{N} \Omega_\mu (e^{-ikz_\mu}\sigma_\mu + e^{ikz_\mu}\sigma_\mu^\dagger), \tag{3}$$

with the position-dependent Rabi frequency $\Omega_\mu = \Omega_0 f(\vec{r}_\mu)$. In addition, $G_{\mu\nu}$ represents the propagator of the dipole-dipole interaction whose real and imaginary parts correspond to the collective decay rate and collective frequency shift, respectively. It is expressed as

$$G_{\mu\nu} = \frac{3\Gamma}{4} e^{i\xi}\left[(1-\cos^2\theta)\frac{i}{\xi} - (1-3\cos^2\theta)\left(\frac{1}{\xi^2} + \frac{i}{\xi^3}\right)\right] \tag{4}$$

and the diagonal term is defined as $G_{\mu\mu} = i\Delta - \Gamma/2$, where $\Delta \equiv \omega_L - \omega_{\text{atom}}$ is the laser detuning, defined as the difference between the laser frequency ω_L and the atomic transition frequency ω_{atom}. Here $\xi = k|\vec{s}_{\mu\nu}| \equiv k|\vec{r}_\mu - \vec{r}_\nu|$ is the atomic spacing and $\cos\theta \equiv \hat{d}\cdot\hat{s}_{\mu\nu}$ is the angle between dipole orientation $\hat{d}$ and relative position vectors $\hat{s}_{\mu\nu}$. The plot in Fig. 1 shows an example of optical depths solved by a full master equation, which depicts a 2×2 atomic array with varying lattice spacing a. We first set up the position distribution $\vec{r}_\mu$ of the atomic array with the given spacing a. Then we calculate all the pair interaction strengths $G_{\mu\nu}$ through Eq. (4). From these, $\mathcal{D}$ can be determined using Eqs. (1)–(3). A significant $\mathcal{D}$ emerges when $a \simeq 0.7\lambda$, showing the enhancement arising from RDDI, in contrast to the noninteracting limit $a \to \infty$. The $\mathcal{D}$ also decreases as $a \to 0$ because of the large collective frequency shift [4] that makes the system differ from the resonant driving condition.

The Hilbert space in solving Eq. (2) grows exponentially and leads to difficulty in calculating the optical response of atomic ensembles even for several atoms. Therefore, a weak-field driving limit $\Omega_0 \to 0$ is often assumed to hugely reduce the exponential computational complexity to polynomial time, neglecting the effects of quantum correlations. From Eq. (1) we see that the light scattering from atoms only involves σ_μ, and using Eqs. (2)–(4) we obtain its steady-state equation of motion

$$0 = G_{\mu\mu}\sigma_\mu + \frac{i\Omega_\mu}{2}e^{-ikz_\mu}(1-2e_\mu) + \sum_{\nu\neq\mu}^{N} G_{\mu\nu}(\sigma_\nu - 2\sigma_\nu e_\mu), \tag{5}$$

where $e_\mu \equiv |e\rangle_\mu\langle e|$ denotes the excited-state population operator. In the weak driving limit, the excited-state population is assumed to be small and thus e_μ and $\sigma_\nu e_\mu$ are neglected. Then the system reduces to N linear coupled equations, which can be solved by calculating the inverse of matrix $G_{\mu\nu}$. However, in this study, we find that the excited-state population can still induce large corrections on light-scattering properties in an atomic ensemble even under a relatively weak driving intensity of $\Omega_0 = 0.1\Gamma$.

Therefore, a more complete theoretical model needs to be applied to include the effect of the excited-state populations and atom-atom correlations. This can be done by including the terms of e_μ and $\sigma_\nu e_\mu$, but these quantities are generally coupled to operators of higher orders, leading to the hierarchy problem [44]. To resolve this, we apply the cumulant expansion method, which truncates higher-order operators to products of lower-order ones by assuming a certain order of the many-body correlation vanishes. For example, we assume the two-body correlation (second-order cumulant) $\langle\sigma_\nu e_\mu\rangle_c \equiv \langle\sigma_\nu e_\mu\rangle - \langle\sigma_\nu\rangle\langle e_\mu\rangle$ to be vanishing in order to relate $\langle\sigma_\nu e_\mu\rangle = \langle\sigma_\nu\rangle\langle e_\mu\rangle$ to first-order cumulants, leading to $3N$ nonlinear coupled equations. Similarly, we can expand the model by truncating higher-order cumulants to second-order ones, thus including the effect of two-body correlations. In general, cumulant expansion can reduce 4^N terms in the full master equation to approximately N^n nonlinearly coupled equations, where n is the order of expansion.

III. MULTIEXCITATION EFFECTS

In this section we demonstrate the light-scattering property from an atomic ensemble beyond the weak-field excitation. We first compare the cumulant expansion model with a full density matrix solution, which indicates the performance and validity of this model. We then investigate a finite driving regime using the same model to reveal how atomic correlations induce saturation in a few-atom system. We further find the same saturation phenomenon in the weak driving regime as we increase the array size in particular shapes, which is not predicted by the linear model. This shows the limitation of the linear model in capturing correct light-scattering properties, and thus other extended models involving higher-order atom-atom correlations will be considered.

A. Comparison to the exact master equation

We use the cumulant expansion as an extension of the linear model. For the first-order expansion, we include the excitation population e_μ and $\sigma_\mu^\dagger$ in the steady-state equations, resulting in $3N$ closed nonlinearly coupled equations. This order of expansion is also known as the mean-field theory [54], as it assumes the density matrix is the product of single-particle states. The equations can be easily solved using Newton's method. Through collecting σ_μ's steady-state equation, the problems transform to finding the root of a

vector-valued function $\vec{F}(\sigma_1, \ldots, \sigma_N) = 0$. The μ component of $\vec{F}$ is the right-hand side of Eq. (5). The computational complexity is the same as the linear model, which grows linearly with the number of atoms N.

For the second-order expansion, we further include all two-body operators such as $\sigma_\nu e_\mu$, $e_\nu e_\mu$, and $\sigma_\nu \sigma_\mu$, as well as their conjugates for $\nu \neq \mu$. The truncation of higher-order cumulants builds up a complex connection throughout the whole coupled equations $\vec{F}(\vec{x})$. Here $\vec{x}$ contains all single and double atomic operators, and each component of $\vec{F}(\vec{x})$ corresponds to the steady-state equation of operator x_i derived from Eq. (2). Due to the complexity of the coupled equations, applying Newton's method becomes challenging, primarily due to the difficulty in computing the inverse of the Jacobian matrix $J_{ij} \equiv \frac{\partial F_i}{\partial x_j}$. Therefore, we employ Broyden's method [55], which offers an iterative approach to approximate the Jacobian matrix through $\vec{x}$. We start with an initial vector $\vec{x}_0$ and an initial guess for the inverse Jacobian matrix J_0^{-1}. We then update their values using the formulas

$$\vec{x}_n = \vec{x}_{n-1} - J_{n-1}^{-1}\vec{F}(\vec{x}_{n-1}), \tag{6}$$

$$J_n^{-1} = J_{n-1}^{-1} + \frac{\vec{s}_n - J_{n-1}^{-1}\vec{y}_n}{\|\vec{y}_n\|^2} \tag{7}$$

for the nth iteration, where $\vec{s}_n = \vec{x}_n - \vec{x}_{n-1}$ and $\vec{y}_n = \vec{F}(\vec{x}_n) - \vec{F}(\vec{x}_{n-1})$. We note that Eq. (6) becomes Newton's method if J_{n-1} is replaced by the exact Jacobian matrix at $\vec{x}_{n-1}$. By repeating the iterations until $\vec{x}_n$ is close to the root $\|\vec{F}(\vec{x}_n)\| \to 0$, we obtain all the steady-state expectation value for these operators.

Figure 2(a) shows the optical depth of the 2×2 atom array under different lattice spacings and driving strengths solved by the full master equation (2). The overall optical depth decreases as the driving intensity increases. The optical depth peak at $a \simeq 0.7\lambda$ also disappears as the driving gets stronger, and a flat $\mathcal{D}$ versus lattice spacing emerges. This is because the saturation in the excited-state population makes the atoms unable to absorb more photons and results in light transparency. In Figs. 2(b)–2(d) we scan the detuning in a range of $\Delta \in [-8\Gamma, 8\Gamma]$ and plot the maximal error for the results calculated by the nth-order truncation $\mathcal{D}_n(\Delta)$ compared to the exact solution $\mathcal{D}_{\rm ex}(\Delta)$ in Fig. 2(a) under a fixed atomic spacing, which is defined as $\max_{\Delta\in[-8\Gamma,8\Gamma]} |\mathcal{D}_n - \mathcal{D}_{\rm ex}|/\mathcal{D}_{\rm ex}$. We have checked that the solution of nonlinear equations converges well so that the errors from numerical precision do not come into play. In Figs. 2(b)–2(d), higher-order truncations in the cumulant expansion method provide more-accurate results. For a weak driving regime at $\Omega_0 = 0.1\Gamma$ in Fig. 2(b), we also compare the results with those using the linear model. The maximal relative error occurs at $a \simeq 0.7\lambda$ and reaches about 10% from the linear model, while the mean-field model only contributes to an error less than 1%. The lattice spacing at which $\mathcal{D}$ is the maximum in Fig. 2(a) coincides with the one where the maximal error emerges in Fig. 2(b). This is due to the subradiant radiation from a periodic atomic configurations at $a \approx 0.8\lambda$ [50], which results in a high $\mathcal{D}$ with significant atom-atom correlations. Therefore, those models that neglect these correlations would present larger errors. For a finite driving as $\Omega_0 \to \Gamma$, Figs. 2(b) and 2(c) show that the second-order expansion provides better results than the first-order one. However, both truncations lead to less accurate results as the lattice spacing becomes smaller at around $a \leqslant 0.5\lambda$. This is expected since in this dense lattice regime RDDI becomes significant, and only a full calculation can faithfully describe the light-scattering properties. In Fig. 2(d), for $\Omega_0 = 1\Gamma$ and $a \lesssim 0.3\lambda$ the error reaches 30% for the mean-field model and 10% for the second-order cumulant expansion method. This indicates that higher-order correlation must be taken into account in the limit of short-distance lattices of atoms and under the strong-field condition $\Omega_0 \gtrsim 1\Gamma$.

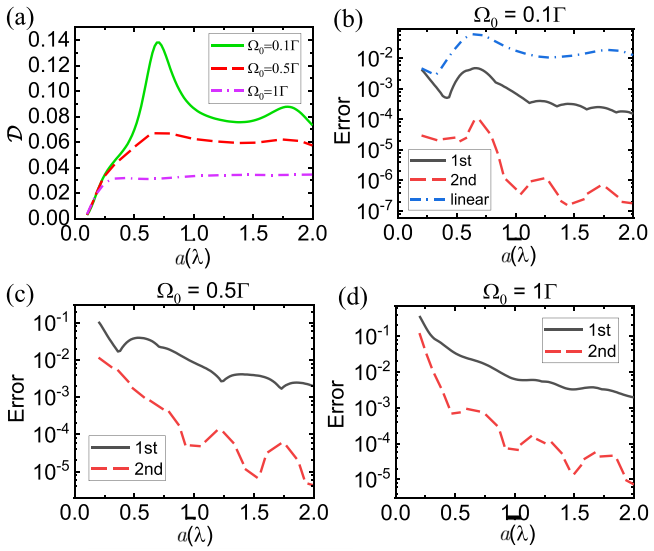

FIG. 2. (a) Exact optical depth and (b)–(d) different models' maximal relative error of the 2×2 array versus various lattice spacings for Rabi frequencies (b) $\Omega_0 = 0.1\Gamma$, (c) $\Omega_0 = 0.5\Gamma$, and (d) $\Omega_0 = 1\Gamma$. For weak driving at $\Omega_0 = 0.1\Gamma$ we also compare the results from the linear model's result. Overall, the solution converges well as we include higher-order cumulants. The only region where the errors of the second-order cumulant expansion exceed 10% is for strong RDDI ($a < 0.3\lambda$) and driving $\Omega_0 = 1\Gamma$. This indicates the regime where higher-order correlations take place.

B. Modification of optical properties beyond weak-field excitation

From the previous results, we can see that the cumulant expansion method provides accurate enough predictions within most of the regimes, except in a dense lattice or under a strong driving field. Here we further explore the optical properties beyond the weak-field excitation. We turn to look at how these additional factors (excited-state population and two-body correlation) beyond weak-field excitations affect the atoms' light-scattering properties as light intensity increases. Figure 3(a) shows the exact $\mathcal{D}$ spectrum of a 2×2 atomic array spaced by 0.5λ under various driving strengths. It is evident that the optical depth decreases as the intensity increases due to the saturation among the atoms, which has been observed and discussed in Fig. 2(a). For these spectra, we fit the profile by the Lorentz function $\mathcal{D}(\Delta) \simeq \mathcal{D}_{\max} \frac{w^2}{4(\Delta-\nu)^2+w^2}$ to obtain the corresponding frequency shift ν and the absorption width w. As Figs. 3(b) and 3(c) show, the light intensity

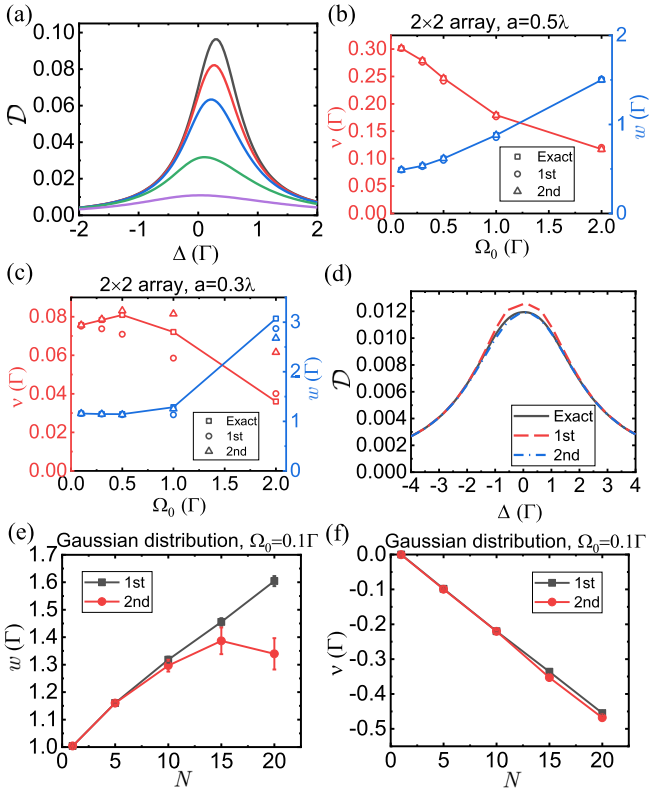

FIG. 3. Linewidth broadening and suppressed line shift for lattice spacings (a) and (b) $a = 0.5\lambda$ and (c) and (d) $a = 0.3\lambda$. In (a), $\mathcal{D}$ decreases as the driving strength increases. The corresponding driving strengths are, from the top curve to the bottom curve, $\Omega_0 = (0.1, 0.3, 0.5, 1, 2)\Gamma$. (e) and (f) Results of a Gaussian-distributed sample with respect to the atom number N. In (b) and (c) the line shift ν and the linewidth w are denoted by red and blue symbols, respectively. (d) Comparison of the optical depth for different cumulant expansion orders with the exact solution at $a = 0.3\lambda$ for $\Omega_0 = 2\Gamma$. The overall profile of the optical depth presents a more-accurate result using the second-order cumulant expansion method. (e) and (f) For randomly distributed samples, a saturation in linewidth is observed only in the second-order expansion. The line shift appears unaffected by the introduction of correlations.

significantly modifies these parameters and induces linewidth broadening and suppressed resonance shift as the intensity gets stronger. For $a = 0.3\lambda$, the frequency shift decreases to half of its value in the weak-field limit and the linewidth broadens to about three times. This can be explained by considering the single-atom case, where the steady-state solution of σ_μ is given by

$$\sigma_\mu = \frac{\Omega_\mu}{2\Delta + i\Gamma}\left(1 + \frac{|\Omega_\mu|^2/2}{\Delta^2 + \frac{\Gamma^2}{4}}\right)^{-1}. \tag{8}$$

The term in large parentheses denotes the nonlinear response exhibited by the dipole in the presence of a finite driving. This term attenuates the light response and depends on the detuning Δ. Specifically, it is suppressed more in the case of a resonant laser ($\Delta = 0$) as compared to the nonresonant light. We can qualitatively interpret this phenomenon in the multiatom system, where the atoms are excited not only by the driving but also by the dipole fields from the other atoms; the total field would lead to the saturation of atoms and the modification of light scattering once its strength is strong enough. Therefore, for strong driving in Figs. 3(b) and 3(c) a similar phenomenon is observed, that the absorption profile broadens and the frequency shift moves toward the resonance condition.

We also show the results fitted from different cumulant expansion orders. In most of the cases, the first-order expansion is enough to identify accurate results for the moderate RDDI as shown in Fig. 3(b). The second-order expansion behaves better than the mean-field model, which is more manifest in Fig. 3(c). In Fig. 3(c) we see that the second-order expansion predicts almost the same absorption width as the exact solution, while some disagreements on frequency shift emerge when the driving strength surpasses Γ. The only exception where the mean-field model has less deviation is near $\Omega_0 = 2\Gamma$ in the considered case of $a = 0.3\lambda$. At this point the first-order cumulant expansion method seems to provide more-accurate results of line shifts, but from Fig. 3(d) we can see that this is just a coincidence since from the overall spectrum, the spectral profile from the second-order cumulant expansion is closer to the exact spectrum.

Instead of focusing on the strong driving regime, we investigate a larger atomic system where the exact solutions are computationally challenging. Figures 3(e) and 3(f) show the absorption width and frequency shift of a Gaussian-distributed atomic cloud as its density increases. The cloud's root-mean-square widths are $(r_x, r_y, r_z) = (0.25\lambda, 0.25\lambda, 1.5\lambda)$, making it cigar shaped, and it is subjected to weak driving. As the density of the cloud increases with the addition of more atoms, deviation in absorption width w emerges between the first- and second-order expansion models. While the mean-field model predicts a linear increase in width, the second-order expansion model exhibits a saturation. However, there is no significant difference between these models concerning the frequency shift ν. This observation may explain the discrepancy between the width predicted by the mean-field model and experimental results [47], showing the significance of correlations in large and dense atomic ensembles. Nonetheless, it fails to account for the disagreement in frequency shift ν, even when considering the influence of high intensities in Figs. 3(c) and 3(d). The inclusion of higher-order correlations may be necessary in denser samples where $N \gg 20$.

C. Saturation of optical depth in a subradiant array

Based on the analysis in Fig. 2, we can identify the regime where the mean-field model predicts well enough the light-scattering properties, where the RDDI is moderate ($a \gtrsim 0.3\lambda$) and the laser intensity is below saturation ($\Omega_0 \lesssim 0.5\Gamma$).

It is expected that an atomic array in the subradiant mode will display a greater deviation from the linear model compared to the superradiant mode under the same driving strength. This deviation arises due to the increasing influence of incoherent scattering within the subradiant mode, which depends on the excitation population and two-body correlations [50]. Such contributions are not accounted for in the linear model. In Fig. 4 we show the trend of $\mathcal{D}$ as the lattice size increases. To explore the limitations of the linear model within subradiant atomic arrays, we select a square

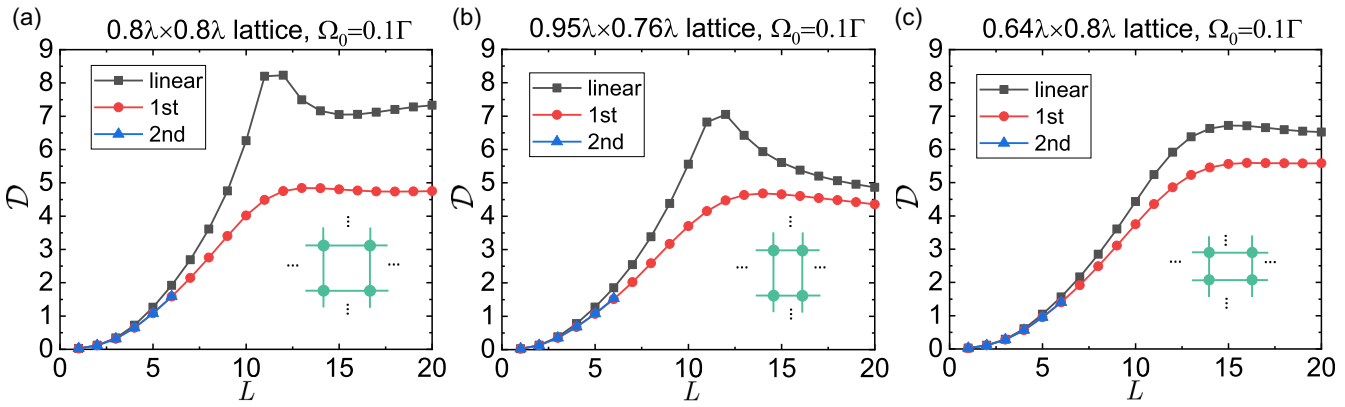

FIG. 4. Optical depth scaling of the $L \times L$ lattice in different shapes. We consider one square array (a) $0.8\lambda \times 0.8\lambda$ and two rectangular arrays (b) $0.95\lambda \times 0.76\lambda$ and (c) $0.64\lambda \times 0.8\lambda$. The deviation between the linear model and cumulant expansion theory increases under the resonant ($\Delta = 0$) and weak driving conditions as the lattice size scales up. The linear model overestimates $\mathcal{D}$, while the cumulant expansion shows a rather smooth and saturated result over L.

array ($0.8\lambda \times 0.8\lambda$) known to exhibit subradiance and a large optical depth when subjected to resonant driving conditions [46]. Our exploration of diverse array shapes also leads to two additional rectangular arrays, both demonstrating subradiant behavior under resonant driving. We choose a relatively weak RDDI region and excite the system in a weak driving condition ($\Omega_0 = 0.1\Gamma$). For a small number of atoms, we also calculate the results by the second-order expansion method as a comparison. We find negligible deviations between the mean-field model and the second-order cumulant expansion method, which indicates the validity of using the mean-field model in a larger system size in the considered parameter regions.

In Fig. 4 it is obvious that the linear model breaks down even under a weak-field excitation when a larger system is considered. We observe that for the linear model, it predicts the largest $\mathcal{D}$ for the case of a $0.8\lambda \times 0.8\lambda$ array comparing the other configurations in the large-L limit, while the mean-field model presents the largest $\mathcal{D}$ in the case of a $0.64\lambda \times 0.8\lambda$ array instead. In the considered parameter regime as shown in Fig. 4, the second-order cumulant expansion overlaps with the mean-field model, which suggests a negligible effect of atom-atom correlations. This indicates that mean-field theory still provides a good model to describe the scattering property of a large ensemble, provided the density is low ($a \gtrsim 0.3\lambda$).

Among these shapes, we also find that the discrepancy between the linear and mean-field models exists in most subwavelength arrays once the number of atoms becomes sufficiently large, especially when driving is resonant with the array's frequency shift. This is because the optical depth peak is dominated by the subradiant mode [46]. Figure 5 illustrates the optical depth for both $0.3\lambda \times 0.9\lambda$ and $0.9\lambda \times 0.3\lambda$ lattices. The detunings $\Delta = -1.4\Gamma$ and 0.66Γ are chosen based on the shift of the optical depth peak in 30×30 arrays. The difference becomes noticeable at very large atomic numbers $L^2 > 400$, which is much larger than those shown in Fig. 4. This shows the limitation of the linear model in predicting large atomic arrays, whose validity also depends on the number of atoms. It demonstrates that the linear model may fail in large atomic systems [40], even when the weak driving condition is met.

IV. CONCLUSION

We have compared the results of light-scattering properties from different models that host different degrees of atom-atom correlations and excitation effect. Through adding successively higher correlations into the steady-state equations, we could obtain an increasingly accurate result with respect to the exact full density matrix solution. Our investigation of the relative errors from this exact solution showed that, for the weak RDDI regime where $a \gtrsim 0.3\lambda$ and the weak driving regime, the first-order cumulant expansion has already given satisfying accuracy for the property of optical depth. Meanwhile, the role of two-body correlations becomes significant as the RDDI transitions into a moderate regime, approximately when $a \lesssim 0.3\lambda$, and under a strong driving condition $\Omega_0 \gtrsim 0.5\Gamma$. When a higher laser intensity is applied, the atomic excitations become saturated, which hugely influences the optical depth. This saturation will cause light transparency and also modifies the light shift and resonance width. In the cases where the atom density is higher, it becomes crucial to account for second-order correlations, as they significantly affect the resonance width. Finally, we also found that this saturation effect can also appear in a subradiant atomic array even when the driving is weak, where the primary contribution to incoherent scattering stems from the excitation population,

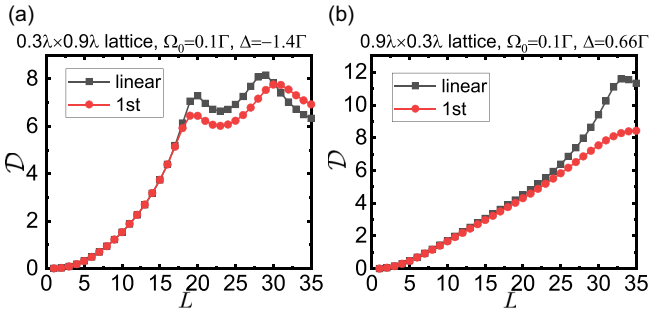

FIG. 5. Optical depth of the (a) $0.3\lambda \times 0.9\lambda$ and (b) $0.9\lambda \times 0.3\lambda$ lattices. The detunings are $\Delta = -1.4\Gamma$ and 0.66Γ. There is no significant deviation between the linear and mean-field models until the number of atoms becomes quite large $L > 20$.

leading to a large deviation from the linear model that is often used for its simplicity. Our results show that the mean-field model could be a good extension of the linear model due to both its accuracy and less computational complexity in most cases. However, for large and dense atomic ensembles, inclusion of second- or higher-order correlations may become necessary, even when the driving is weak. This presents a challenge in the study of light-matter interacting systems.

ACKNOWLEDGMENTS

We are grateful for insightful discussions with F. Robicheaux. We acknowledge support from the National Science and Technology Council, Taiwan, under Grants No. 112-2112-M-001-079-MY3 and No. NSTC-112-2119-M-001-007. We are also grateful for support from TG 1.2 of NCTS at NTU.

[1] K. Hammerer, A. S. Sørensen, and E. S. Polzik, Quantum interface between light and atomic ensembles, Rev. Mod. Phys. **82**, 1041 (2010).

[2] P. Forn-Díaz, L. Lamata, E. Rico, J. Kono, and E. Solano, Ultrastrong coupling regimes of light-matter interaction, Rev. Mod. Phys. **91**, 025005 (2019).

[3] A. de la Torre, D. M. Kennes, M. Claassen, S. Gerber, J. W. McIver, and M. A. Sentef, *Colloquium:* Nonthermal pathways to ultrafast control in quantum materials, Rev. Mod. Phys. **93**, 041002 (2021).

[4] R. H. Lehmberg, Radiation from an N-atom system. I. General formalism, Phys. Rev. A **2**, 883 (1970).

[5] N. E. Rehler and J. H. Eberly, Superradiance, Phys. Rev. A **3**, 1735 (1971).

[6] R. Bonifacio and L. A. Lugiato, Cooperative radiation processes in two-level systems: Superfluorescence, Phys. Rev. A **11**, 1507 (1975).

[7] R. H. Dicke, Coherence in spontaneous radiation processes, Phys. Rev. **93**, 99 (1954).

[8] E. Sierra, S. J. Masson, and A. Asenjo-Garcia, Dicke superradiance in ordered lattices: Dimensionality matters, Phys. Rev. Res. **4**, 023207 (2022).

[9] M. O. Araújo, I. Krešić, R. Kaiser, and W. Guerin, Superradiance in a large and dilute cloud of cold atoms in the linear-optics regime, Phys. Rev. Lett. **117**, 073002 (2016).

[10] W. Guerin, M. O. Araújo, and R. Kaiser, Subradiance in a large cloud of cold atoms, Phys. Rev. Lett. **116**, 083601 (2016).

[11] H. H. Jen, M.-S. Chang, and Y.-C. Chen, Cooperative single-photon subradiant states, Phys. Rev. A **94**, 013803 (2016).

[12] H. H. Jen, Cooperative single-photon subradiant states in a three-dimensional atomic array, Ann. Phys. (NY) **374**, 27 (2016).

[13] A. Asenjo-Garcia, M. Moreno-Cardoner, A. Albrecht, H. J. Kimble, and D. E. Chang, Exponential improvement in photon storage fidelities using subradiance and "selective radiance" in atomic arrays, Phys. Rev. X **7**, 031024 (2017).

[14] H. H. Jen, Phase-imprinted multiphoton subradiant states, Phys. Rev. A **96**, 023814 (2017).

[15] H. H. Jen, M.-S. Chang, and Y.-C. Chen, Cooperative light scattering from helical-phase-imprinted atomic rings, Sci. Rep. **8**, 9570 (2018).

[16] H. H. Jen, Directional subradiance from helical-phase-imprinted multiphoton states, Sci. Rep. **8**, 7163 (2018).

[17] J. A. Needham, I. Lesanovsky, and B. Olmos, Subradiance-protected excitation transport, New J. Phys. **21**, 073061 (2019).

[18] M. Moreno-Cardoner, D. Plankensteiner, L. Ostermann, D. E. Chang, and H. Ritsch, Subradiance-enhanced excitation transfer between dipole-coupled nanorings of quantum emitters, Phys. Rev. A **100**, 023806 (2019).

[19] M. Moreno-Cardoner, R. Holzinger, and H. Ritsch, Efficient nano-photonic antennas based on dark states in quantum emitter rings, Opt. Express **30**, 10779 (2022).

[20] A. Cipris, N. A. Moreira, T. S. do Espirito Santo, P. Weiss, C. J. Villas-Boas, R. Kaiser, W. Guerin, and R. Bachelard, Subradiance with saturated atoms: Population enhancement of the long-lived states, Phys. Rev. Lett. **126**, 103604 (2021).

[21] S. Davidson, F. A. Pollock, and E. Gauger, Eliminating radiative losses in long-range exciton transport, PRX Quantum **3**, 020354 (2022).

[22] J. Ruostekoski, Cooperative quantum-optical planar arrays of atoms, Phys. Rev. A **108**, 030101 (2023).

[23] R. Holzinger, J. Peter, S. Ostermann, H. Ritsch, and S. Yelin, Harnessing quantum emitter rings for efficient energy transport and trapping, Opt. Quantum **2**, 57 (2024).

[24] S. D. Jenkins, J. Ruostekoski, J. Javanainen, S. Jennewein, R. Bourgain, J. Pellegrino, Y. R. P. Sortais, and A. Browaeys, Collective resonance fluorescence in small and dense atom clouds: Comparison between theory and experiment, Phys. Rev. A **94**, 023842 (2016).

[25] R. T. Sutherland and F. Robicheaux, Collective dipole-dipole interactions in an atomic array, Phys. Rev. A **94**, 013847 (2016).

[26] A. Glicenstein, G. Ferioli, N. Šibalić, L. Brossard, I. Ferrier-Barbut, and A. Browaeys, Collective shift in resonant light scattering by a one-dimensional atomic chain, Phys. Rev. Lett. **124**, 253602 (2020).

[27] A. Cidrim, A. Piñeiro Orioli, C. Sanner, R. B. Hutson, J. Ye, R. Bachelard, and A. M. Rey, Dipole-dipole frequency shifts in multilevel atoms, Phys. Rev. Lett. **127**, 013401 (2021).

[28] L. Chomaz, L. Corman, T. Yefsah, R. Desbuquois, and J. Dalibard, Absorption imaging of a quasi-two-dimensional gas: A multiple scattering analysis, New J. Phys. **14**, 055001 (2012).

[29] D. E. Chang, J. S. Douglas, A. González-Tudela, C.-L. Hung, and H. J. Kimble, *Colloquium*: Quantum matter built from nanoscopic lattices of atoms and photons, Rev. Mod. Phys. **90**, 031002 (2018).

[30] M. Zhang, L. Feng, M. Li, Y. Chen, L. Zhang, D. He, G. Guo, G. Guo, X. Ren, and D. Dai, Supercompact photonic quantum logic gate on a silicon chip, Phys. Rev. Lett. **126**, 130501 (2021).

[31] T. Chanelière, D. N. Matsukevich, S. D. Jenkins, T. A. B. Kennedy, M. S. Chapman, and A. Kuzmich, Quantum telecommunication based on atomic cascade transitions, Phys. Rev. Lett. **96**, 093604 (2006).

[32] N. Rivera and I. Kaminer, Light–matter interactions with photonic quasiparticles, Nat. Rev. Phys. **2**, 538 (2020).

[33] T. Laurent, Y. Todorov, A. Vasanelli, A. Delteil, C. Sirtori, I. Sagnes, and G. Beaudoin, Superradiant emission from a collective excitation in a semiconductor, Phys. Rev. Lett. **115**, 187402 (2015).

[34] A. M. Kaufman and K.-K. Ni, Quantum science with optical tweezer arrays of ultracold atoms and molecules, Nat. Phys. **17**, 1324 (2021).

[35] G. Ferioli, A. Glicenstein, F. Robicheaux, R. T. Sutherland, A. Browaeys, and I. Ferrier-Barbut, Laser-driven superradiant ensembles of two-level atoms near Dicke regime, Phys. Rev. Lett. **127**, 243602 (2021).

[36] J. Keaveney, A. Sargsyan, U. Krohn, I. G. Hughes, D. Sarkisyan, and C. S. Adams, Cooperative lamb shift in an atomic vapor layer of nanometer thickness, Phys. Rev. Lett. **108**, 173601 (2012).

[37] J. Pellegrino, R. Bourgain, S. Jennewein, Y. R. P. Sortais, A. Browaeys, S. D. Jenkins, and J. Ruostekoski, Observation of suppression of light scattering induced by dipole-dipole interactions in a cold-atom ensemble, Phys. Rev. Lett. **113**, 133602 (2014).

[38] J. Geng, G. T. Campbell, J. Bernu, D. B. Higginbottom, B. M. Sparkes, S. M. Assad, W. P. Zhang, N. P. Robins, P. K. Lam, and B. C. Buchler, Electromagnetically induced transparency and four-wave mixing in a cold atomic ensemble with large optical depth, New J. Phys. **16**, 113053 (2014).

[39] K. J. Kemp, S. J. Roof, M. D. Havey, I. M. Sokolov, D. V. Kupriyanov, and W. Guerin, Optical-depth scaling of light scattering from a dense and cold atomic ^{87}Rb gas, Phys. Rev. A **101**, 033832 (2020).

[40] L. Corman, J. L. Ville, R. Saint-Jalm, M. Aidelsburger, T. Bienaimé, S. Nascimbène, J. Dalibard, and J. Beugnon, Transmission of near-resonant light through a dense slab of cold atoms, Phys. Rev. A **96**, 053629 (2017).

[41] J. Rui, D. Wei, A. Rubio-Abadal, S. Hollerith, J. Zeiher, D. M. Stamper-Kurn, C. Gross, and I. Bloch, A subradiant optical mirror formed by a single structured atomic layer, Nature (London) **583**, 369 (2020).

[42] M. Mücke, E. Figueroa, J. Bochmann, C. Hahn, K. Murr, S. Ritter, C. J. Villas-Boas, and G. Rempe, Electromagnetically induced transparency with single atoms in a cavity, Nature (London) **465**, 755 (2010).

[43] S. J. Masson and A. Asenjo-Garcia, Atomic-waveguide quantum electrodynamics, Phys. Rev. Res. **2**, 043213 (2020).

[44] J. Ruostekoski and J. Javanainen, Quantum field theory of cooperative atom response: Low light intensity, Phys. Rev. A **55**, 513 (1997).

[45] E. Shahmoon, D. S. Wild, M. D. Lukin, and S. F. Yelin, Cooperative resonances in light scattering from two-dimensional atomic arrays, Phys. Rev. Lett. **118**, 113601 (2017).

[46] R. J. Bettles, S. A. Gardiner, and C. S. Adams, Enhanced optical cross section via collective coupling of atomic dipoles in a 2D array, Phys. Rev. Lett. **116**, 103602 (2016).

[47] S. Jennewein, M. Besbes, N. J. Schilder, S. D. Jenkins, C. Sauvan, J. Ruostekoski, J.-J. Greffet, Y. R. P. Sortais, and A. Browaeys, Coherent scattering of near-resonant light by a dense microscopic cold atomic cloud, Phys. Rev. Lett. **116**, 233601 (2016).

[48] S. J. Roof, K. J. Kemp, M. D. Havey, and I. M. Sokolov, Observation of single-photon superradiance and the cooperative Lamb shift in an extended sample of cold atoms, Phys. Rev. Lett. **117**, 073003 (2016).

[49] F. Robicheaux and D. A. Suresh, Intensity effects of light coupling to one- or two-atom arrays of infinite extent, Phys. Rev. A **108**, 013711 (2023).

[50] L. A. Williamson and J. Ruostekoski, Optical response of atom chains beyond the limit of low light intensity: The validity of the linear classical oscillator model, Phys. Rev. Res. **2**, 023273 (2020).

[51] R. Kubo, Generalized cumulant expansion method, J. Phys. Soc. Jpn. **17**, 1100 (1962).

[52] F. Robicheaux and D. A. Suresh, Beyond lowest order mean-field theory for light interacting with atom arrays, Phys. Rev. A **104**, 023702 (2021).

[53] O. Rubies-Bigorda, S. Ostermann, and S. F. Yelin, Characterizing superradiant dynamics in atomic arrays via a cumulant expansion approach, Phys. Rev. Res. **5**, 013091 (2023).

[54] K. J. Kusmierek, S. Mahmoodian, M. Cordier, J. Hinney, A. Rauschenbeutel, M. Schemmer, P. Schneeweiss, J. Volz, and K. Hammerer, Higher-order mean-field theory of chiral waveguide QED, SciPost Phys. Core **6**, 041 (2023).

[55] A. Baran, A. Bulgac, M. M. Forbes, G. Hagen, W. Nazarewicz, N. Schunck, and M. V. Stoitsov, Broyden's method in nuclear structure calculations, Phys. Rev. C **78**, 014318 (2008).